Testing the Running of non-Gaussianity through the CMB μ-distortion and the Halo Bias

Matteo Biagetti, Hideki Perrier, Antonio Riotto and Vincent Desjacques

Université de Genève, Department of Theoretical Physics and Center for Astroparticle Physics (CAP), 24 quai E. Ansermet, CH-1211 Geneva 4, Switzerland

Abstract

The primordial non-Gaussianity parameters $f_{\rm NL}$ and $\tau_{\rm NL}$ may be scale-dependent. We investigate the capability of future measurements of the CMB μ-distortion, which is very sensitive to small scales, and of the large-scale halo bias to test the running of local non-Gaussianity. We show that, for an experiment such as PIXIE, a measurement of the μ-temperature correlation can pin down the spectral indices $n_{f_{\rm NL}}$ and $n_{\tau_{\rm NL}}$ to values of the order of 0.3 if $f_{\rm NL} = 20$ and $\tau_{\rm NL} = 5000$. A similar value can be achieved with an all-sky survey extending to redshift $z \sim 1$. In the particular case in which the two spectral indices are equal, as predicted in models where the cosmological perturbations are generated by a single field other than the inflaton, then the 1-σ error on the scale-dependence of the non-linearity parameters goes down to 0.2.

1 Introduction

Detecting a possible primordial source of non-Gaussianity (NG) in the cosmological perturbations is one of the main targets of current and future experiments measuring the properties of the Cosmic Microwave Background (CMB) anisotropies and the large-scale structure. Indeed, measuring a certain level of NG in the three- (bispectrum) and four-point (trispectrum) correlator of the perturbations opens up a unique window into the physics of inflation which is believed to be the period during which such fluctuations are quantum-mechanically generated [1]. The current constraints on NG come from the measurement of the CMB anisotropy bispectrum [2] and from the properties of the clustering of galaxies which has been identified to be a powerful probe of NG thanks to the fact that NG introduces a scale-dependent bias between the power spectra of halos and dark matter [3,4].

Most of the attention in the literature has been devoted to the so-called "local" model of NG, where the NG is defined in terms of the primordial gravitational potential $\Phi(\vec{x})$ as

$$\Phi(\vec{x}) = \phi_{\rm G}(\vec{x}) + f_{\rm NL}\Big[\phi^2_{\rm G}(\vec{x}) - \langle\phi^2_{\rm G}(\vec{x})\rangle\Big]. \tag{1}$$

The corresponding bispectrum and trispectrum are given by

$$B_\Phi(k_1,k_2,k_3) = 2f_{\rm NL}\Big[P_\phi(k_1)P_\phi(k_2) + 2 \text{ cyc.}\Big], \tag{2}$$

$$T_\Phi(k_1,k_2,k_3,k_4) = \frac{25}{9}\tau_{\rm NL}\Big[P_\phi(k_1)P_\phi(k_2)P_\phi(k_{13}) + 11 \text{ cyc.}\Big], \tag{3}$$

where $P_\phi(k)$ is the power spectrum of the gravitational potential. This type of NG is generated in multifield inflationary models where the cosmological perturbation is sourced by light scalar fields other than the inflaton. The corresponding perturbations are both scale invariant and special conformally invariant [5,6]. The parameter $f_{\rm NL}$ is currently constrained to be in the range (32 ± 21) by WMAP [2] and (28 ± 23) by the large-scale structure [7], while the parameter $\tau_{\rm NL}$ needs to be in the range $(-0.6 < \tau_{\rm NL}/10^4 < 3.3)$ as inferred from the WMAP 5-year data [8]. Measuring the amplitudes of both the bispectrum and the trispectrum is extremely interesting as, if only one degree of freedom is responsible for the perturbations, then there is a well-defined relation between the NG parameters, $\tau_{\rm NL} = \left(\frac{6}{5}f_{\rm NL}\right)^2$. On the contrary, if more than one field is responsible for the cosmological perturbations generated through the inflationary dynamics, then there exists an inequality, $\tau_{\rm NL} > \left(\frac{6}{5}f_{\rm NL}\right)^2$ [6,9,10]. To which extent future measurements of the scale-dependence of halo bias can test multi-field inequality has been the subject of Ref. [11].

Even though the definitions (2) and (3) are widely used to model NG in the primordial perturbations, it is just the first step one can make on this matter. One, more general, definition of the bispectrum and trispectrum could include a scale-dependence in the non-linearity parameters $f_{\rm NL}$ and $\tau_{\rm NL}$. This step is well-motivated by the theoretical predictions of some models [12–16]. The running with physical scale of the NG parameters $f_{\rm NL}$ and $\tau_{\rm NL}$ has been the subject of an intense recent research [17–24].

To account for the running of $f_{\rm NL}$ in its full generality one can adopt for example the parametrization used in Ref. [25] (see also Ref. [14])

$$B_\Phi(k_1,k_2,k_3) = 2\left[\xi_{f_{\rm NL}}(k_3)\xi_m(k_1)\xi_m(k_2)P_\phi(k_1)P_\phi(k_2) + \text{cyc.}\right], \tag{4}$$

where

$$\xi_{f_{\rm NL},m}(k) = \xi_{f_{\rm NL},m}(k_0)\left(\frac{k}{k_0}\right)^{n_{f_{\rm NL},m}}. \tag{5}$$

Here $\xi_{f_{\rm NL}}(k)$ parametrizes the (self-)interactions of the fields and $\xi_m(k)$ the ratio of the contribution of each field. From this general parametrization, we can also easily extend the one for the trispectrum

$$T_\Phi(k_1,k_2,k_3,k_4) = \frac{25}{9}\left[\xi_{\tau_{\rm NL}}(k_3,k_4)\xi_m(k_1)\xi_m(k_2)\xi_m(k_{13})P_\phi(k_1)P_\phi(k_2)P_\phi(k_{13}) + \text{cyc.}\right], \tag{6}$$

where

$$\xi_{\tau_{\rm NL}}(k_i,k_j) = \xi_{\tau_{\rm NL}}(k_0)\left(\frac{k_ik_j}{k_0^2}\right)^{n_{\tau_{\rm NL}}}. \tag{7}$$

In the single-field limit, $\xi_{\tau_{\rm NL}}(k_i,k_j) = \frac{36}{25}\xi_{f_{\rm NL}}(k_i)\xi_{f_{\rm NL}}(k_j)$ and $\xi_m(k) = 1$. According to this parametrization, in the case of a multi-field inflation, we have three free parameters, $n_{f_{\rm NL}}$, n_m and $n_{\tau_{\rm NL}}$, which describe the scale dependence of the non-linearity parameters $f_{\rm NL}$ and $\tau_{\rm NL}$ and of the dimensionless power spectra. In order to decrease the complexity of the analysis, from now on we make the assumption that n_m is significantly much smaller than unity. By doing so, we are left with the following parametrization of the non-linear parameters

$$f_{\rm NL}(k) = f^*_{\rm NL}\left(\frac{k}{k_*}\right)^{n_{f_{\rm NL}}}, \tag{8}$$

and

$$\tau_{\rm NL}(k_i,k_j) = \tau^*_{\rm NL}\left(\frac{k_i k_j}{k_*^2}\right)^{n_{\tau_{\rm NL}}}. \tag{9}$$

CMB information alone, in the event of a significant detection of the NG component, corresponding to $f_{\rm NL}=50$ for the local model, is able to determine $n_{f_{\rm NL}}$ with a 1-σ uncertainty of about 0.1 for the Planck mission [17]. A local bias analysis performed in the same Ref. [17] showed that high-redshift surveys ($z>1$) covering a large fraction of the sky corresponding to a volume of about $100\,h^{-3}$ Gpc^3 might provide a 1-σ error on the running $f_{\rm NL}$ parameter of the order of $0.4(50/f_{\rm NL})$. On the other hand, using the WMAP temperature maps, a constraint on the running of the scale-dependent parameter $f_{\rm NL}$ has been recently obtained in Ref. [26] to be $n_{f_{\rm NL}}=0.30(+1.9)(-1.2)$ at 95% confidence, marginalized over the amplitude $f^*_{\rm NL}$. To the best of our knowledge, no forecasts for the running of the trispectrum parameter $\tau_{\rm NL}$ exist in the literature. In fact, in the case in which the perturbations are sourced by a single field, then a well-defined relation between the running spectral indices holds,

$$n_{f_{\rm NL}} = n_{\tau_{\rm NL}} \tag{10}$$

and the indices are therefore not independent. In this paper we will assume that $f_{\rm NL}$ and $\tau_{\rm NL}$, and therefore their spectral indices too, are not related to each other, thus leaving open the possibility that the perturbations are originated from a multi-field scenario.

The goal of this paper is to provide some useful forecasts on the spectral indices $n_{f_{\rm NL}}$ and $n_{\tau_{\rm NL}}$ from the possible physical imprints that NG can leave on the the CMB μ-distortion and the halo bias. Measurements of the μ-type distortion of the CMB spectrum provide the unique opportunity to probe these scales over the unexplored range from 50 to 10^4 Mpc^{-1} and it has been recently pointed out that correlations between μ-distortion and temperature anisotropies can be used to test Gaussianity at these very small scales. In particular the μ-temperature cross correlation is proportional to the very squeezed limit of the local primordial bispectrum and hence measures $f_{\rm NL}$, while the μ-μ is proportional to the primordial trispectrum and measures $\tau_{\rm NL}$ [27] (see also [28]). Being the μ-distortion localized at small scales, we expect it to be very sensitive to the possible running of the NG parameters $f_{\rm NL}$ and $\tau_{\rm NL}$. This will be studied in section 2. In section 3 we will study the effect of running NG parameters onto the halo bias, taking into account the running of the trispectrum amplitude as well. Our conclusions will be presented in section 4. In all illustrations, the cosmology is a flat ΛCDM Universe with normalisation $\sigma_8=0.803$, Hubble constant $h_0=0.701$ and matter content $\Omega_{\rm m}=0.279$.

2 CMB μ-distortion

The goal of this section is to compute the effect of the running NG onto the CMB μ-distortion. The latter is caused by the energy injection originated by the dissipation of acoustic waves through the Silk damping as they re-enter the horizon and start oscillating. The interesting property is that this effect is related to primordial perturbation scales of $50 \lesssim k\,{\rm Mpc} \lesssim 10^4$ which are not accessible from CMB anisotropies observations.

At early times ($z \gg z_{\mu,i} \equiv 2\times 10^6$), the content of the universe can be described by a photon-baryon fluid in thermal equilibrium which has a black-body spectrum. This equilibrium is achieved mainly through elastic and double Compton scattering. However, at later times ($z_{\mu,f} \equiv 5\times 10^4 \lesssim z \lesssim z_{\mu,i}$), double Compton scattering is no longer efficient whereas the single Compton scattering still provides equilibrium. The photon number density is however frozen and only the frequency of the photons can be changed. It can be shown that any energy injection in the photon-baryon fluid will distort the spectrum by the creation of a chemical potential μ. The photon number density per frequency interval is then $n(\nu)=(e^{x+\mu(x)}-1)^{-1}$, where $x\equiv h\nu/(k_BT)$. The parameter μ due to damping of acoustic waves can then be expressed in terms of the primordial power spectrum [29]. Using the Bose-Einstein distribution plus the fact that the total number of photons is constant, for an amount of energy (density) released into the plasma $\delta E/E$, one finds that $\mu \simeq 1.4\delta E/E$, where

$$\frac{\delta E}{E} \simeq \frac{1}{4}\,\langle\delta^2_\gamma(\vec{x})\rangle\Big|^{z_{\mu,i}}_{z_{\mu,f}}, \tag{11}$$

and $\langle\delta^2_\gamma(\vec{x})\rangle$ represents the photon energy density fluctuation averaged over one period of the acoustic oscillations. As the modes of interest re-enter the horizon during the radiation phase, one finally finds

$$\mu(\vec{x}) \simeq 4.6 \int \frac{\mathrm{d}^3k_1 \mathrm{d}^3k_2}{(2\pi)^6} \zeta_{\vec{k}_1}\zeta_{\vec{k}_2} e^{i\vec{k}_+\cdot\vec{x}} W\left(\frac{\vec{k}_+}{k_s}\right) \langle \cos(k_1 r)\cos(k_2 r)\rangle_p \left[e^{-(k_1^2+k_2^2)/k_D^2},\right]_{z_{\mu,f}}^{z_{\mu,i}}. \tag{12}$$

where $\zeta(\vec{x}) = 5\Phi(\vec{x})/3$ describes curvature perturbations, $\vec{k}_\pm \equiv \vec{k}_1 \pm \vec{k}_2$ and in order to account for the fact that the distortion arises from a thermalization process, one uses a top-hat filter in real space $W(\vec{x})$, which smears the dissipated energy over a volume of radius $k_{D,f}^{-1} \lesssim k_s^{-1}$, where $k_D(z)$ is the diffusion momentum scale

$$k_D(z) \simeq 4.1 \cdot 10^{-6}(1+z)^{3/2}\mathrm{Mpc}^{-1}. \tag{13}$$

We proceed by computing the correlations between μ-distortion and temperature anisotropy as well as $\mu\mu$ self correlation as done in [27], but allowing for a running of $f_{\rm NL}$ and $\tau_{\rm NL}$ given by Eq. (8) and (9). The curvature perturbation bispectrum in the squeezed limit ($k_3 \ll k_1 \sim k_2$) is expressed as

$$\langle \zeta_{\vec{k}_1}\zeta_{\vec{k}_2}\zeta_{\vec{k}_3}\rangle = (2\pi)^3\delta^3(\vec{k}_1+\vec{k}_2+\vec{k}_3)\frac{12}{5} f_{\rm NL}(k_-/2)P(k_-/2)P(k_+). \tag{14}$$

The temperature-μ correlation therefore reads[1]

$$\begin{aligned} C_\ell^{\mu T} &= -6.1\pi \frac{9}{25} f_{\rm NL}^* b \frac{\Delta_\zeta^4(k_p)}{\ell(\ell+1)} \ln\left(\frac{k_{D,i}}{k_{D,f}}\right) \\ &\simeq -2.2\times 10^{-16} f_{\rm NL}^* \frac{b}{\ell(\ell+1)}, \end{aligned} \tag{15}$$

where the primordial curvature spectrum is defined by $\langle \zeta_{\vec{k}_1}\zeta_{\vec{k}_2}\rangle = (2\pi)^3\delta^3(\vec{k}_1+\vec{k})2\pi^2\Delta_\zeta^2(k_1)/k_1^3$ with $\Delta_\zeta^2(k_p) = 2.4\times 10^{-9}$ at the pivot scale $k_p \equiv 0.002\,\mathrm{Mpc}^{-1}$ [2]. The parameter b is defined by

$$\begin{aligned} \frac{b}{\ell(\ell+1)} &\equiv \frac{2}{\ln\left(\frac{k_{D,i}}{k_{D,f}}\right)} \int \mathrm{d}\ln k_+ \, j_\ell(k_+ r_\ell)^2 W\left(\frac{k_+}{k_s}\right) \\ &\times \int \mathrm{d}\ln k_- \left(\frac{k_-}{2k_*}\right)^{n_{f_{\rm NL}}} \frac{\Delta_\zeta^2(k_-/2)\Delta_\zeta^2(k_+)}{\Delta_\zeta^4(k_p)} \left[e^{-k_-^2/(2k_D^2(z))}\right]_{z_{\mu,f}}^{z_{\mu,i}}. \end{aligned} \tag{16}$$

The μ-distortion is created during the period between $z_{\mu,i} = 2\times 10^6$ and $z_{\mu,f} = 5\times 10^4$ which implies $k_{D,i} \simeq 11600$ Mpc^{-1} and $k_{D,f} \simeq 46$ Mpc^{-1}. For a weak scale dependence $\Delta_\zeta^2(k) = \Delta_\zeta^2(k_p)(k/k_p)^{n_s-1}$ we obtain

$$b \simeq \frac{1}{\ln\left(\frac{k_{D,i}}{k_{D,f}}\right)} \frac{1}{n_s + n_{f_{\rm NL}} - 1} \left(\frac{1}{\sqrt{2}k_p}\right)^{n_s-1} \left(\frac{1}{\sqrt{2}k_*}\right)^{n_{f_{\rm NL}}} \left[k_D(z)^{n_s+n_{f_{\rm NL}}-1}\right]_{z_{\mu,f}}^{z_{\mu,i}}. \tag{17}$$

If we take the same pivot for $f_{\rm NL}$ as for the primordial spectrum, $k_* = k_p$, the equation above becomes the same expression as for a constant $f_{\rm NL} = f_{\rm NL}^*$ but with a shifted spectral index n_s replaced by $(n_s + n_{f_{\rm NL}})$. This shows explicitly that we recover the scale invariant result for $n_{f_{\rm NL}} = 0$ and we have $b \simeq 1 + 10(n_s + n_{f_{\rm NL}} - 1)$ for $(n_s + n_{f_{\rm NL}} - 1) \simeq 0$.

Using the trispectrum in the collapsed limit ($\vec{k}_{12} \sim 0$)

$$\langle \zeta_{\vec{k}_1}\zeta_{\vec{k}_2}\zeta_{\vec{k}_3}\zeta_{\vec{k}_4}\rangle = (2\pi)^3\delta^3(\vec{k}_1+\vec{k}_2+\vec{k}_3+\vec{k}_4)4\tau_{\rm NL}(k_-/2,k_3)P(k_-/2)P(k_+)P(k_3), \tag{18}$$

we obtain the NG contribution to the μ-distortion self-correlation

$$\begin{aligned} C_\ell^{\mu\mu} &= 42\pi\tau_{\rm NL}^* \widetilde{b} \frac{\Delta_\zeta^6(k_p)}{\ell(\ell+1)} \ln^2\left(\frac{k_{D,i}}{k_{D,f}}\right) \\ &\simeq 5.6\times 10^{-23}\tau_{\rm NL}^* \frac{\widetilde{b}}{\ell(\ell+1)}, \end{aligned} \tag{19}$$

[1] To compute the temperature anisotropies we adopt the same approximation as in Ref. [27], that is the Sachs-Wolfe approximation. Based on the findings in Ref. [28], where the full radiation transfer function was adopted, we expect an overall decrease of the signal-to-noise ratio of order of 40%. Later in the text, we also point out that the change of the pivot scale amounts to corrections of the order of 30%.

where

$$\widetilde{b} \equiv \frac{2l(l+1)}{\ln^2\left(\frac{k_{D,i}}{k_{D,f}}\right)} \int \mathrm{d}\ln k_+ \mathrm{d}\ln k_- \,\mathrm{d}\ln k_3\, j_\ell(k_+ r_\ell)^2 W\left(\frac{k_+}{k_s}\right) \times \left(\frac{k_- k_3}{2k_*^2}\right)^{n_{\tau_{\rm NL}}} \frac{\Delta^2_\zeta(k_-/2)\Delta^2_\zeta(k_+)\Delta^2_\zeta(k_3)}{\Delta^6_\zeta(k_p)} \left[e^{-k_-^2/(2k_D^2)}\right]^{z_{\mu,i}}_{z_{\mu,f}} \left[e^{-2k_3/(2k_D^2)}\right]^{z_{\mu,i}}_{z_{\mu,f}}$$

$$\simeq \frac{1}{\ln^2\left(\frac{k_{D,i}}{k_{D,f}}\right)} \left(\frac{1}{n_{\tau_{\rm NL}}+n_s-1}\right)^2 \left(\frac{1}{\sqrt{2}k_p}\right)^{2(n_s-1)} \left(\frac{1}{\sqrt{2}k_*}\right)^{2n_{\tau_{\rm NL}}} \left(\left[k_D(z)^{n_{\tau_{\rm NL}}+n_s-1}\right]^{z_{\mu,i}}_{z_{\mu,f}}\right)^2. \quad (20)$$

This is just b^2 with the index $n_{f_{\rm NL}}$ replaced by $n_{\tau_{\rm NL}}$ and it corresponds to the result of a constant $\tau_{\rm NL} = \tau^*_{\rm NL}$ with n_s replaced by $(n_s + n_{\tau_{\rm NL}})$. We recover the scale-invariant result for $n_{\tau_{\rm NL}} = 0$. The behaviour of the parameters b and $\widetilde{b}$ is shown on Fig. 1.

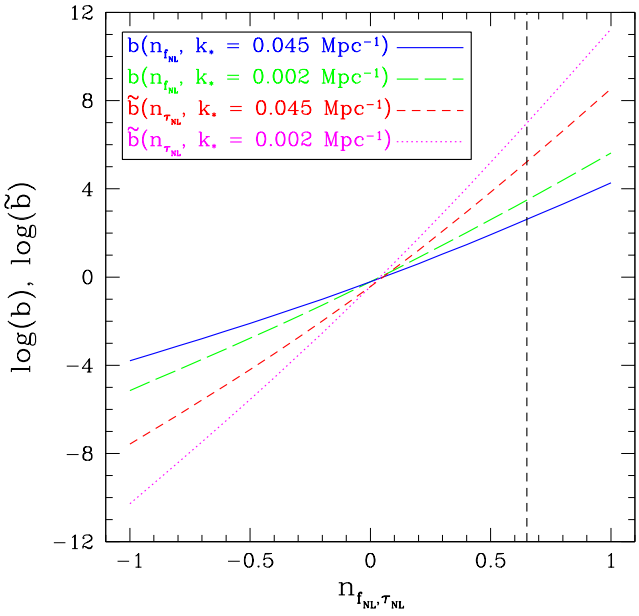

Figure 1: Value of the parameters $b(n_{f_{\rm NL}})$ and $\widetilde{b}(n_{\tau_{\rm NL}})$ for two different pivot scales k_* and $n_s = 0.96$. The dashed line shows the maximal value of $n_{f_{\rm NL}}$ (and $n_{\tau_{\rm NL}}$), for which the approximation (25) is correct.

Having computed the key parameters b and $\widetilde{b}$, we proceed by estimating the signal-to-noise ratio to estimate the values of $n_{f_{\rm NL}}$ and $n_{\tau_{\rm NL}}$ measurable from the μ-distortion assuming that the amplitude $f^*_{\rm NL}$ and $\tau^*_{\rm NL}$ are known from some other experiments. In general the signal-to-noise ratio for variables λ_i is defined in terms of the Fisher matrix as [30]

$$\frac{S}{N} \equiv \sqrt{\lambda_i F_{ij} \lambda_j}. \quad (21)$$

In the case of only one variable, it reduces to $S/N = \lambda\sqrt{F} = \lambda/\sigma_\lambda$. In our case, to measure the spectral index $n_{f_{\rm NL}}$ we can adopt the Fisher matrix

$$F = \sum_{\ell\geq 2} \frac{1}{\sigma^2_{C_\ell^{\mu T}}} \left(\frac{\partial C_\ell^{\mu T}}{\partial n_{f_{\rm NL}}}\right)^2, \quad (22)$$

while for the spectral index $n_{\tau_{\rm NL}}$ we adopt the Fisher matrix

$$F = \sum_{\ell\geq 2} \frac{1}{\sigma^2_{C_\ell^{\mu\mu}}} \left(\frac{\partial C_\ell^{\mu\mu}}{\partial n_{\tau_{\rm NL}}}\right)^2. \quad (23)$$

The noise for μ-distortion can be modelled assuming a Gaussian beam experiment [31] by

$$C_\ell^{\mu\mu,N} \simeq w_\mu^{-1} e^{\ell^2/\ell^2_{\rm max}}, \quad (24)$$

where $\ell_{\rm max}$ is the maximum multipole fixed by the experiment's beam size and w_μ is the sensitivity to μ. For the PIXIE experiment [32], $\ell_{\rm max} = 84$ and $w_\mu^{-1/2} = \sqrt{4\pi} \times 10^{-8}$. We also approximate the variance of the C_ℓ's by

$$\begin{aligned}\sigma^2_{C_\ell^{\mu T}} &= \langle (C_\ell^{\mu T})^2 \rangle - \langle C_\ell^{\mu T} \rangle^2 \\ &= \frac{1}{2\ell+1}\left((C_\ell^{\mu\mu} + C_\ell^{\mu\mu,N})(C_\ell^{TT} + C_\ell^{TT,N}) + (C_\ell^{\mu T})^2 \right) \\ &\simeq \frac{1}{2\ell+1} C_\ell^{TT} C_\ell^{\mu\mu,N} \end{aligned} \tag{25}$$

and

$$\sigma^2_{C_\ell^{\mu\mu}} \simeq \frac{2}{2\ell+1} (C_\ell^{\mu\mu,N})^2, \tag{26}$$

where we used that $C_\ell^{TT} \gg C_\ell^{TT,N}$, $C_\ell^{\mu\mu,N} \gg C_\ell^{\mu\mu}$ and $C_\ell^{TT} C_\ell^{\mu\mu,N} \gg (C_\ell^{\mu T})^2$.[2]

The signal-to-noise for $n_{f_{\rm NL}}$ at fixed $f^*_{\rm NL}$ is given by

$$\begin{aligned}\left(\frac{S}{N}\right)_{n_{f_{\rm NL}}} &= n_{f_{\rm NL}} / \sigma_{n_{f_{\rm NL}}}(n_{f_{\rm NL}}) \\ &= n_{f_{\rm NL}} \sqrt{w_\mu \ln\left(\frac{l_{\rm max}}{2}\right)} 11\sqrt{\pi} \Delta^3_\zeta(k_p) f^*_{\rm NL} \left(\frac{1}{\sqrt{2}k_*}\right)^{n_{f_{\rm NL}}} \left(\frac{1}{\sqrt{2}k_p}\right)^{n_s-1} \left(\frac{1}{n_{f_{\rm NL}} + n_s - 1}\right) \\ &\times \left(\left(\ln\left(\frac{1}{\sqrt{2}k_*}\right) - \frac{1}{n_{f_{\rm NL}} + n_s - 1} \right) \left[k_D^{n_{f_{\rm NL}} + n_s - 1} \right]^{z_{\mu,i}}_{z_{\mu,f}} + \left[\ln(k_D) k_D^{n_{f_{\rm NL}} + n_s - 1} \right]^{z_{\mu,i}}_{z_{\mu,f}} \right), \end{aligned} \tag{27}$$

whereas the signal-to-noise for $n_{\tau_{\rm NL}}$ at fixed $\tau^*_{\rm NL}$ is

$$\begin{aligned}\left(\frac{S}{N}\right)_{n_{\tau_{\rm NL}}} &= n_{\tau_{\rm NL}} 30\pi w_\mu \Delta^6_\zeta(k_p) \tau^*_{\rm NL} \ln^2\left(\frac{k_{D,i}}{k_{D,f}}\right) \\ &\times \left(\ln\left(\frac{1}{\sqrt{2}k_*}\right) - \frac{1}{n_{\tau_{\rm NL}} + n_s - 1} + \frac{\left[\ln(k_D) k_D^{n_{\tau_{\rm NL}} + n_s - 1} \right]^{z_{\mu,i}}_{z_{\mu,f}}}{\left[k_D^{n_{\tau_{\rm NL}} + n_s - 1} \right]^{z_{\mu,i}}_{z_{\mu,f}}} \right) \widetilde{b}(n_{\tau_{\rm NL}}, k_*). \end{aligned} \tag{28}$$

The left plot of Fig. 2 shows $n_{f_{\rm NL}}(f^*_{\rm NL})$ at $(S/N)_{n_{f_{\rm NL}}} = 1$. An amplitude $f^*_{\rm NL} \lesssim 10^2$ enables to detect $n_{f_{\rm NL}} \gtrsim 0.3$, at least with the PIXIE experiment. Notice also that the dependence on the choice of k_* is relatively low. The right plot of figure 2 shows $n_{\tau_{\rm NL}}(\tau^*_{\rm NL})$ at $(S/N)_{n_{\tau_{\rm NL}}} = 1$. Values of $\tau^*_{\rm NL} \lesssim 10^5$ enable to detect $n_{\tau_{\rm NL}} \gtrsim 0.3$, again with the PIXIE experiment.

In the single field case, we can use both the temperature-μ-distortion correlation $C^{\mu T}$ or the μ-distortion self-correlation $C^{\mu\mu}$ to measure $n_{f_{\rm NL}}$. As shown in Fig. 3, $C^{\mu T}$ allows to detect lower values of $n_{f_{\rm NL}}$.

3 Halo bias

Let us now turn to the effect of running NG parameters onto the halo bias [17, 20–22, 25, 35]. The halo bias power spectrum with Gaussian initial conditions can be simply expressed at lowest order in terms of a linear (Eulerian) bias parameter

$$P_h(k) = \left(b_1^E\right)^2 P_m(k), \tag{29}$$

where $P_m(k)$ is the dark matter power spectrum. The effect of primordial non-Gaussianity on the halo bias can be accurately predicted from a peak-background split [33–37]. As shown in [35], the non-Gaussian contribution to the linear bias induced by a non-zero primordial N-point function is

$$\begin{aligned}\Delta b_1(k) &= \frac{4}{(N-1)!} \frac{\mathcal{F}_s^{(N)}(k,z)}{\mathcal{M}_s(k,z)} \\ &\times \left[b_{N-2}\delta_c + b_{N-3}\left(N - 3 + \frac{d\ln \mathcal{F}_s^{(N)}(k,z)}{d\ln\sigma_s} \right) \right], \end{aligned} \tag{30}$$

[2] Using the explicit expressions above, we find that this condition is verified provided that $(f^*_{\rm NL} b)^2$, $\tau^*_{\rm NL}\widetilde{b} < 10^7 \ell^2$. We consider the pivots $k_* = 0.002\,{\rm Mpc}^{-1}$ and $k_* = 0.064h\,{\rm Mpc}^{-1} \simeq 0.045\,{\rm Mpc}^{-1}$. The former corresponds to the pivot k_p of the primordial spectrum and the latter to the best pivot value from [26]. For $\tau^*_{\rm NL} \sim (f^*_{\rm NL})^2 \sim 10^4$ and $\ell \sim 10^2$, we find that the approximation (25) is valid for $n_{f_{\rm NL}}, n_{\tau_{\rm NL}} \lesssim (0.65 - 0.85)$ depending on the pivot k_*, see Fig. 1 which presents the values of b and $\widetilde{b}$ as function of the indices $n_{f_{\rm NL}}$ and $n_{\tau_{\rm NL}}$ for the two pivots. One should be aware that in the multiple field case, $\tau^*_{\rm NL}$ is larger than $((6/5)f^*_{\rm NL})^2$, so the approximation becomes worse. In general, it seems reasonable to trust our estimation up to $n_{f_{\rm NL}}, n_{\tau_{\rm NL}} \simeq 0.5$.

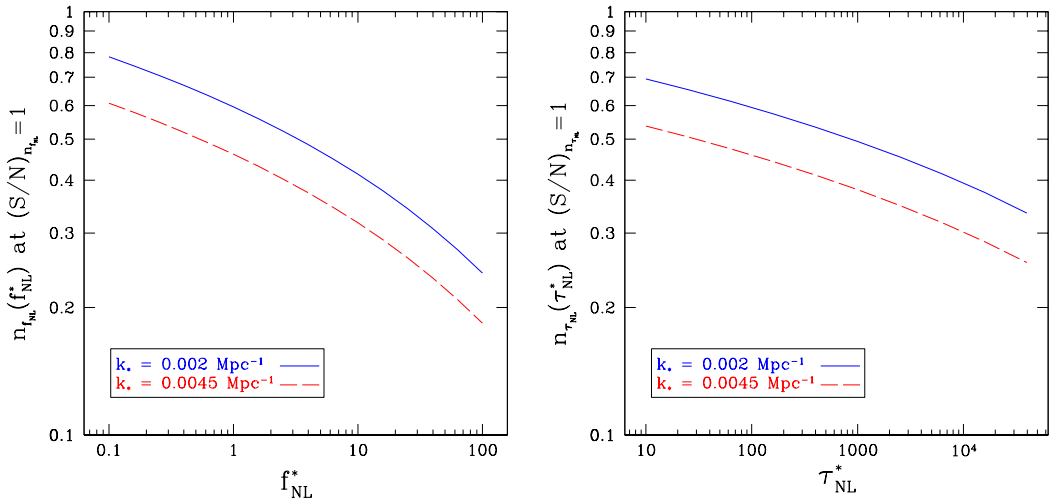

Figure 2: Left: The spectral index $n_{f_{\rm NL}}$ as function of $f^*_{\rm NL}$ at $(S/N)_{n_{f_{\rm NL}}} = 1$. Right: The spectral index $n_{\tau_{\rm NL}}$ as function of $\tau^*_{\rm NL}$ at $(S/N)_{n_{\tau_{\rm NL}}} = 1$. Both plots are made for two different pivot scales k_*, using $k_p = 0.002\,{\rm Mpc}^{-1}$ and $n_s = 0.96$ for PIXIE.

where b_N are Lagrangian bias parameters, $\delta_c \sim 1.68$ is the critical threshold for (spherical) collapse and σ_s is the rms variance of the density field at redshift z smoothed on the (small) scale R_s of a halo. While this expression assumes a universal mass function, it can be generalized to take into account deviations from universality in actual halo mass functions [37].

The linear matter density contrast $\delta_{\vec{k}}(z)$ is related to the curvature perturbation $\Phi_{\vec{k}}$ during matter domination via the Poisson equation. The latter can be expressed as the Fourier space relation $\delta_{\vec{k}}(z) = \mathcal{M}(k,z)\,\Phi_{\vec{k}}$, where

$$\mathcal{M}(k,z) \equiv \frac{2}{3}\frac{D(z)}{\Omega_m H_0^2}\,T(k)\,k^2. \tag{31}$$

Here, $T(k)$ is the matter transfer function, Ω_m and H_0 are the matter density in critical units and the Hubble rate today, and $D(z)$ is the linear growth rate. $\mathcal{M}_s$ is a shorthand for $\mathcal{M}(k,z)W(kR_s)$, where $W(kR_s)$ is a spherically symmetric window function (we adopt a top-hat filter throughout this paper). Furthermore,

$$\begin{aligned}\mathcal{F}_s^{(N)}(k,z) = \frac{1}{4\sigma_s^2 P_\phi(k)}\left[\prod_{i=1}^{N-2}\int\frac{{\rm d}^3k_1}{(2\pi)^3}\,\mathcal{M}_s(k_i,z)\right]\mathcal{M}_s(q,z)\\ \times\,\xi_\Phi^{(N)}(\vec{k}_1,\cdots,\vec{k}_{N-2},\vec{q},\vec{k})\end{aligned} \tag{32}$$

is a projection factor whose k-dependence is dictated by the exact shape of the N-point function $\xi_\Phi^{(N)}$ of the gravitational potential. For the local constant-$f_{\rm NL}$ model, the factor $\mathcal{F}_s^{(3)}$ is equal to $f_{\rm NL}$ in the low k-limit (squeezed limit), so that the logarithmic derivative of $\mathcal{F}_s^{(N)}$ with respect to the rms variance σ_s of the small-scale density field vanishes on large scales. However, this does not hold for scale-dependent primordial non-Gaussianity. In this case, we use expressions (4) and (6) for the bispectrum and trispectrum to evaluate the derivative of $\mathcal{F}_s^{(N)}$ with respect to σ_s.

For generic primordial 3- and 4-point functions, the non-Gaussian halo power spectrum reads

$$\begin{aligned}P_h(k) \;=\; &\left[(b_1^E)^2 + 4b_1^E b_1\delta_c\frac{\mathcal{F}(n_{f_{\rm NL}},M)}{\mathcal{M}_R(k)} + \frac{25}{27}b_1^E\left[b_2\delta_c\sigma_R^2 + b_1\left(1+\frac{d\ln\mathcal{T}_1}{d\ln\sigma_R}\right)\right]\frac{\mathcal{T}_1(n_{\tau_{\rm NL}},M)}{\mathcal{M}_R(k)} + \right.\\ &\left. + \frac{25}{9}b_1^2\delta_c^2\frac{\mathcal{T}_2(n_{\tau_{\rm NL}},M)}{\mathcal{M}_R^2(k)}\right]P_m(k)\,,\end{aligned} \tag{33}$$

where, on large scales, the last term in the square brackets can generate stochasticity between the halo and

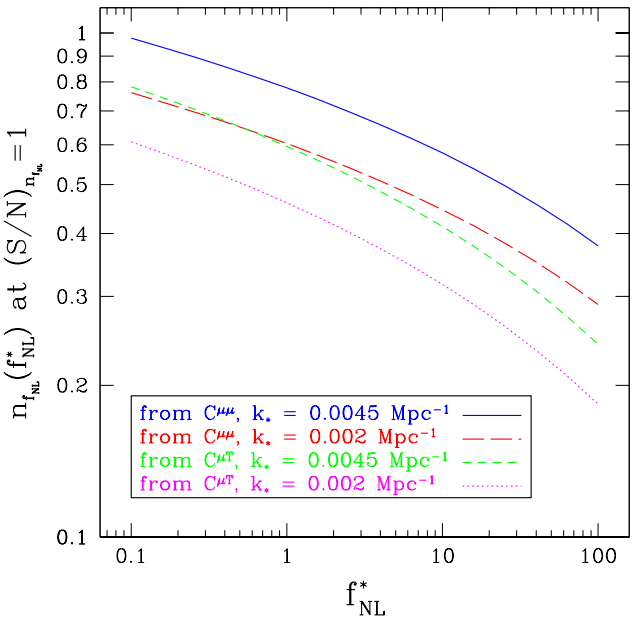

Figure 3: Using the temperature-μ-distortion correlation $C^{\mu T}$ allows to detect lower values of $n_{f_{\rm NL}}$ than using the μ-distortion self-correlation $C^{\mu\mu}$ in the single field case. The spectral index $n_{f_{\rm NL}}$ at $(S/N)_{n_{f_{\rm NL}}}$ is shown for two different pivot scales k_*, using $k_p = 0.002\,{\rm Mpc}^{-1}$ and $n_s = 0.96$ for PIXIE.

mass density fields if $\tau_{\rm NL}$ is different from $(6f_{\rm NL}/5)^2$ [38–41]). We have defined the quantities

$$\mathcal{F}(n_{f_{\rm NL}}, M) = \frac{1}{\sigma_R^2}\int \frac{{\rm d}q}{2\pi^2} q^2 \mathcal{M}_R^2(q) P(q) f_{\rm NL}(q), \tag{34}$$

$$\mathcal{T}_1(n_{\tau_{\rm NL}}, M) = \frac{6}{\sigma_R^4}\int \frac{{\rm d}^3q_1 {\rm d}^3q_2}{(2\pi)^6} \mathcal{M}_R(q_1)\mathcal{M}_R(q_2)\mathcal{M}_R(q_{12}) P(q_1)P(q_2)\tau_{\rm NL}(q_1, q_{12}), \tag{35}$$

$$\mathcal{T}_2(n_{\tau_{\rm NL}}, M) = \frac{1}{\sigma_R^4}\int \frac{{\rm d}q_1 {\rm d}q_2}{(2\pi^2)^2} q_1^2 q_2^2 \mathcal{M}_R^2(q_1)\mathcal{M}_R^2(q_1) P(q_1)P(q_2)\tau_{\rm NL}(q_1, q_2)\,. \tag{36}$$

We have used the definitions (8) and (9) to obtain these expressions. We have also emphasized the dependence on the parameters $n_{f_{\rm NL}}$ and $n_{\tau_{\rm NL}}$, as well as the halo mass M which, for the top-hat filter, is related to the smoothing radius R through $R = (3M/4\pi)^{1/3}$. The values of $f^*_{\rm NL}$ and $\tau^*_{\rm NL}$ at the pivot wavenumber $k_* = 0.045$ Mpc^{-1} are assumed to be known. In the particular case of scale-independent $f_{\rm NL}$ and $\tau_{\rm NL}$, i.e. $n_{f_{\rm NL}} = n_{\tau_{\rm NL}} = 0$, we recover the expressions given in Refs. [38] and [41].

In order to assess the ability of forthcoming experiments to probe the scale dependence of the non-linearity parameters $f_{\rm NL}$ and $\tau_{\rm NL}$ through a measurement of the large scale bias, we use the Fisher information content on $f_{\rm NL}$ and $\tau_{\rm NL}$ (see e.g. [17,20–23,25] for application to the scale-dependence of $f_{\rm NL}$) in the two-point statistics of halos and dark matter in Fourier space.

Computing the Fisher information requires knowledge of the covariance matrix of the halo samples,

$$C_h(k, M, z) = b^2(k, M, z) P_m(k) + \frac{1}{\bar{n}}, \tag{37}$$

where $\bar{n}$ is the mean number density of the survey. In order to constrain $n_{f_{\rm NL}}$ and $n_{\tau_{\rm NL}}$, we assume that we have already measured $f^*_{\rm NL}$ and $\tau^*_{\rm NL}$. Moreover, since we are interested in investigating the possibility of a detection of the spectral indices, we take $n_{f_{\rm NL}} = n_{\tau_{\rm NL}} = 0$ throughout as fiducial values. The Fisher matrix is defined as follows

$$\mathcal{F}_{ij} = V_{\rm surv}\, f_{\rm sky} \int \frac{{\rm d}k\, k^2}{2\pi^2} \frac{1}{2C_h^2} \frac{\partial C_h}{\partial\theta_i} \frac{\partial C_h}{\partial\theta_j}, \tag{38}$$

where θ_i are the parameters whose error we wish to forecast, $V_{\rm surv}$ is the surveyed volume and $f_{\rm sky}$ is the fraction of the sky observed. The integral over the momenta runs from $k_{\rm min} = 2\pi/(V_{\rm surv})^{1/3}$ to $k_{\rm max} = 0.03\,{\rm Mpc}^{-1}/h$, above which the non-Gaussian bias becomes smaller than contributions from second-order bias and nonlinear gravitational evolution. For illustration, we adopt the specifications of a wide-angle, high-redshift survey such as BigBOSS or EUCLID: $V_{\rm surv} f_{\rm sky} = 50\ {\rm Gpc}^3/h^3$ at median redshift $z = 0.7$. Furthermore, we ignore redshift evolution and assume that all the surveyed volume is at the median redshift.

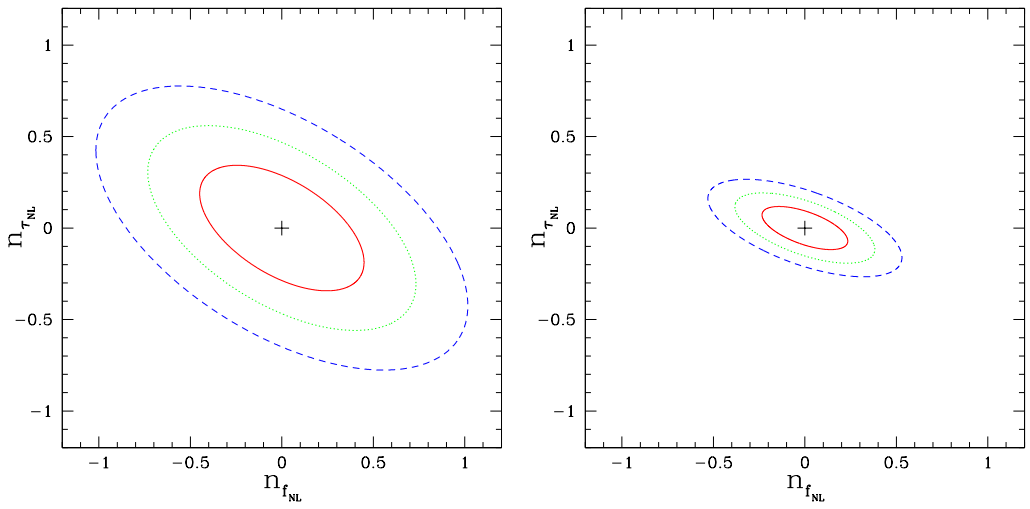

Figure 4: Confidence ellipses obtained by the population of tracers considered with halos with mass larger than $M = 10^{13} M\odot/h$, assuming $f^*_{\rm NL} = 20$ and $\tau^*_{\rm NL} = 5 \times 10^3$ (left) and $f^*_{\rm NL} = 50$ and $\tau^*_{\rm NL} = 5 \times 10^4$ (right).

Table 1: 1-σ errors for the population considered in the two different sets of $f^*_{\rm NL}$ and $\tau^*_{\rm NL}$ in Fig.4.

$f^*_{\rm NL}$	$\tau^*_{\rm NL}$	$\sigma_{n_{f_{\rm NL}}}$	$\sigma_{n_{\tau_{\rm NL}}}$
20	5×10^3	0.30	0.23
50	5×10^4	0.15	0.08

We compute the uncertainties on $n_{f_{\rm NL}}$ and $n_{\tau_{\rm NL}}$ from a single population of tracers consisting of all halos of mass larger than $10^{13} M\odot/h$. Computing the Lagrangian bias factors from a Sheth-Tormen mass function [42] leads a linear and quadratic Lagrangian bias $b_1 = 0.7$ and $b_2 = -0.4$. We take the number density to be $\bar{n} = 10^{-4}$ Mpc$^3/h^3$.

Fig. 4 shows the resulting 68, 95 and 99% confidence contours for the parameters $n_{f_{\rm NL}}$ and $n_{\tau_{\rm NL}}$ when we assume two different combinations of $f^*_{\rm NL}$ and $\tau^*_{\rm NL}$. The 1-σ errors are displayed in Table 1. In the specific case in which only one degree of freedom is responsible for the perturbations, we can use the relation $\tau_{\rm NL}(k_i, k_j) = \frac{36}{25} f_{\rm NL}(k_i) f_{\rm NL}(k_j)$, which leaves us with only one parameter, $n_{f_{\rm NL}}$, describing the scale dependence of the primordial NG. The 1-σ error for $n_{f_{\rm NL}}$ as a function of $f^*_{\rm NL}$ is shown in Fig. 5. This result can be compared with those of previous work. For a fiducial value of $f^*_{\rm NL} = 50$ in particular, we find an error of $\Delta n_{f_{\rm NL}} \sim 0.2$ in the case of multi-field models, and $\Delta n_{f_{\rm NL}} \sim 0.1$ in the case of single-field models. For single-field models, this is a factor of $\mathcal{O}(3)$ lower than the forecast error found in Ref. [17] for a survey like EUCLID. We attribute this difference to the fact that we have considered the higher-order term $\mathcal{O}(f^2_{\rm NL})$ in the halo bias and to the parametrization $f_{\rm NL}(K) = f_{\rm NL}(k_*)(K^{1/3}/k_*)^{n_{f_{\rm NL}}}$ considered in Ref. [17] for the running of $f_{\rm NL}$. In this regards, note that $K \equiv k_1 k_2 k_3$ gives a contribution to the scaling of the external momentum, leading to a suppression (for a positive $n_{f_{\rm NL}}$) or enhancement (for a negative $n_{f_{\rm NL}}$) of the signal with respect to our parametrization in Eq. (8).[3]. We have checked that, if we use the parametrization and restrict ourselves to the $\mathcal{O}(f_{\rm NL})$ contribution to the halo bias, we are able to reproduce their results. As noted in the introduction, the parametrization used in this paper seems to be motivated by various theoretical predictions (see for example [14, 25]).

4 Conclusion

Even a tiny level of non-Gaussianity in the cosmological perturbations can tell us a lot about the dynamics of the inflationary Universe. In this paper, we have focused on local non-Gaussianity, which is a generic prediction of multifield inflationary models where cosmological perturbations are sourced by light scalar fields other than the inflaton. We have considered the possibility that the non-linear parameter $f_{\rm NL}$ is scale-dependent and, extending the previous literature, we have also assumed that $\tau_{\rm NL}$ may be scale-dependent. This is an unavoidable consequence when only a single field other than the inflaton generates the perturbation as the spectral indices

[3]Determining $n_{f_{\rm NL}}$ through μ-distortion using the parametrization of Ref. [17] also leads to a deterioration of the S/N ratio. The parameter b is approximated by Eq. (17) with $n_{f_{\rm NL}}$ replaced by $2n_{f_{\rm NL}}/3$. The correlation $C^{\mu T}$ is decreased by a factor of about $\exp(-c\, n_{f_{\rm NL}})$ with $c \simeq 3$, 4 for $k_* = 0.002, 0.045\,{\rm Mpc}^{-1}$ respectively, relative to the parametrization Eq.(8). Correspondingly, the error $\sigma_{n_{f_{\rm NL}}}$ is increased by about $\frac{3}{2}\exp(c\, n_{f_{\rm NL}})$

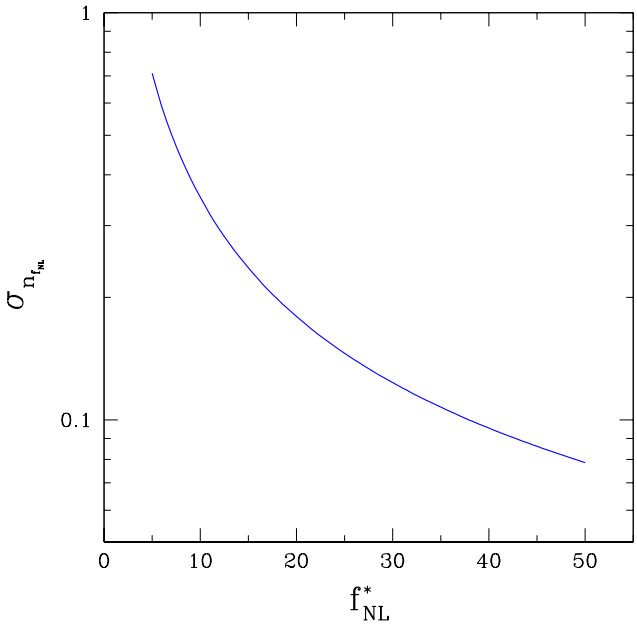

Figure 5: 1-σ error predictions for $n_{f_{\rm NL}}$ as a function of $f^*_{\rm NL}$ at the pivot point $k_* = 0.045\,{\rm Mpc}^{-1}$ for the population considered in the case of one-single field models.

$n_{f_{\rm NL}}$ and $n_{\tau_{\rm NL}}$ are equal. We have considered two possible probes of a running non-Gaussianity. First, we have exploited the fact that future measurements of the CMB μ-distortion will be very sensitive to small scales, thereby enhancing the effect of a (blue) tilt of the NG parameters. Second, we have assessed the ability of a large-scale galaxy survey to constrain the scale dependence of $f_{\rm NL}$ and $\tau_{\rm NL}$ imprinted in the non-Gaussian halo bias. Assuming the detection of a non-vanishing $f_{\rm NL}$ and $\tau_{\rm NL}$, we find both for a CMB experiment like PIXIE and a large-scale survey like EUCLID that the spectral indices could be measured with an accuracy of $\mathcal{O}(0.3)$ for $f_{\rm NL} = 20$ and $\tau_{\rm NL} = 5000$. In the case of a measurement of the scale-dependent halo bias, this limit could be improved by suitably combining the information from several tracers (e.g. [43]).

Acknowledgments

M.B. and V.D. are supported by the Swiss National Science Foundation (SNSF). H.P. and A.R. are supported by the Swiss National Science Foundation (SNSF), project "The non-Gaussian Universe" (project number: 200021140236).

References

[1] For a review, see N. Bartolo, E. Komatsu, S. Matarrese and A. Riotto, Phys. Rept. **402**, 103 (2004) arXiv:0406398 [astro-ph.CO].

[2] E. Komatsu *et al.* [WMAP Collaboration], Astrophys. J. Suppl. **192**, 18 (2011) arXiv:1001.4538 [astro-ph.CO].

[3] N. Dalal, O. Dore, D. Huterer and A. Shirokov, Phys. Rev. D **77**, 123514 (2008) arXiv:0710.4560 [astro-ph.CO].

[4] For a review, see, V. Desjacques and U. Seljak, Adv. Astron. **2010**, 908640 (2010) arXiv:1006.4763 [astro-ph.CO].

[5] P. Creminelli, Phys. Rev. D **85**, 041302 (2012) arXiv:1108.0874 [hep-th].

[6] A. Kehagias and A. Riotto, Nucl. Phys. B **864**, 492 (2012) arXiv:1205.1523 [hep-th]; A. Kehagias and A. Riotto, Nucl. Phys. B **868**, 577 (2013) arXiv:1210.1918 [hep-th].

[7] A. Slosar, C. Hirata, U. Seljak, S. Ho and N. Padmanabhan, JCAP **0808**, 031 (2008) [arXiv:0805.3580 [astro-ph]]; N. Afshordi and A. J. Tolley, Phys. Rev. D **78**, 123507 (2008) arXiv:0806.1046 [astro-ph.CO].

[8] J. Smidt, A. Amblard, C. T. Byrnes, A. Cooray, A. Heavens and D. Munshi, Phys. Rev. D **81**, 123007 (2010) arXiv:1004.1409 [astro-ph.CO].

[9] T. Suyama and M. Yamaguchi, Phys. Rev. D **77**, 023505 (2008) arXiv:0709.2545 [astro-ph.CO].

[10] G. Tasinato, C. T. Byrnes, S. Nurmi and D. Wands, arXiv:1207.1772 [hep-th].

[11] M. Biagetti, V. Desjacques and A. Riotto, arXiv:1208.1616 [astro-ph.CO], to appear in MNRAS.

[12] X. Chen, Phys. Rev. D **72**, 123518 (2005) arXiv:0507053 [astro-ph.CO].

[13] J. Khoury and F. Piazza, JCAP **0907**, 026 (2009) arXiv:0811.3633 [hep-th].

[14] C. T. Byrnes, M. Gerstenlauer, S. Nurmi, G. Tasinato and D. Wands, JCAP **1010**, 004 (2010) arXiv:1007.4277 [astro-ph.CO].

[15] A. Riotto and M. S. Sloth, Phys. Rev. D **83**, 041301 (2011) arXiv:1009.3020 [astro-ph.CO].

[16] C. T. Byrnes, K. Enqvist, S. Nurmi and T. Takahashi, JCAP **1111**, 011 (2011) arXiv:1108.2708 [astro-ph.CO].

[17] E. Sefusatti, M. Liguori, A. P. S. Yadav, M. G. Jackson and E. Pajer, JCAP **0912**, 022 (2009) arXiv:0906.0232 [astro-ph.CO].

[18] Q. -G. Huang, JCAP **1011**, 026 (2010) [Erratum-ibid. **1102**, E01 (2011)] arXiv:1008.2641 [astro-ph.CO].

[19] Q. -G. Huang, JCAP **1012**, 017 (2010) arXiv:1009.3326 [astro-ph.CO].

[20] A. Becker, D. Huterer and K. Kadota, JCAP **1101**, 006 (2011) arXiv:1009.4189 [astro-ph.CO].

[21] A. Becker, D. Huterer and K. Kadota, arXiv:1206.6165 [astro-ph.CO].

[22] M. LoVerde, A. Miller, S. Shandera and L. Verde, JCAP **0804**, 014 (2008) arXiv:0711.4126 [astro-ph.CO].

[23] T. Giannantonio and C. Porciani, Mon. Not. Roy. Astron. Soc. **422** (2012) 2854-2877 arXiv:1109.0958 [astro-ph.CO].

[24] I. Agullo and S. Shandera, JCAP **1209**, 007 (2012) arXiv:1204.4409 [astro-ph.CO].

[25] S. Shandera, N. Dalal and D. Huterer, JCAP **1103**, 017 (2011) arXiv:1010.3722 [astro-ph.CO].

[26] A. Becker and D. Huterer, Phys. Rev. Lett. **109**, 121302 (2012) arXiv:1207.5788 [astro-ph.CO].

[27] E. Pajer and M. Zaldarriaga, Phys. Rev. Lett. **109**, 021302 (2012) arXiv:1201.5375 [astro-ph.CO]].

[28] J. Ganc and E. Komatsu, Phys. Rev. D **86**, 023518 (2012) arXiv:1204.4241 [astro-ph.CO].

[29] J. Chluba and R. A. Sunyaev, arXiv:1109.6552 [astro-ph.CO].

[30] F. James, Statistical Methods in Experimental Physics, 2nd ed. (World Scientific, 2006).

[31] S. Dodelson, "Modern Cosmology" (Academix New York, 2003).

[32] A. Kogut, *et al.*, J. Cosmol. Astropart. Phys. 07 (2011) 025.

[33] A. Slosar, JCAP **0903**, 004 (2009) arXiv:0808.0044 [astro-ph].

[34] F. Schmidt and M. Kamionkowski, Phys. Rev. D **82**, 103002 (2010) arXiv:1008.0638 [astro-ph.CO].

[35] V. Desjacques, D. Jeong and F. Schmidt, Phys. Rev. D **84**, 063512 (2011) arXiv:1105.3628 [astro-ph.CO].

[36] K. M. Smith, S. Ferraro and M. LoVerde, JCAP **1203**, 032 (2012) arXiv:1106.0503 [astro-ph.CO].

[37] R. Scoccimarro, L. Hui, M. Manera and K. C. Chan, Phys. Rev. D **85**, 083002 (2012) arXiv:1108.5512 [astro-ph.CO].

[38] J.-O. Gong and S. Yokoyama S., 2011, Mon. Not. Roy. Astron. Soc. **417**, L79 arXiv:1106.4404 [astro-ph.CO].

[39] D. Tseliakhovich, C.M. Hirata, A. Slosar, Phys. Rev. D **82**, 043531 (2010) arXiv:1004.3302 [astro-ph.CO].

[40] D. Baumann, S. Ferraro, D. Green and K. M. Smith, arXiv:1209.2173 [astro-ph.CO].

[41] S. Yokoyama and T. Matsubara, arXiv:1210.2495 [astro-ph.CO].

[42] R.K. Sheth, H.J. Mo and G. Tormen, Mon. Not. Roy. Astron. Soc. **323**, 1 (2001) arXiv:9907024 [astro-ph.CO].

[43] N. Hamaus, U. Seljak and V. Desjacques, Phys. Rev. D **84**, 083509 (2011) arXiv:1104.2321 [astro-ph.CO].